12th Int. Particle Acc. Conf. IPAC2021, Campinas, SP, Brazil JACoW Publishing
ISBN: 978-3-95450-214-1 ISSN: 2673-5490 doi:10.18429/JACoW-IPAC2021-TUPAB081

DESIGN OF THE BEAM DISTRIBUTION SYSTEM OF SHINE*

S. Chen†, X. Fu, H. Deng, R. Wang, M. Gu
Shanghai Advanced Research Institute, CAS, Shanghai, China

Abstract

The SHINE project is a high repetition rate, high brightness hard X-ray free electron laser facility which is under construction in Shanghai, China. For simultaneously operation of the three undulator lines of SHINE, it is necessary to use a beam distribution system between the linac and undulator lines. In this work, we present the schematic design of the beam distribution system, describe the current lattice design and preliminary S2E simulation results.

INTRODUCTION

As the first hard X-ray free electron laser facilities in China, SHINE project is now under construction in Shanghai [1]. High quality electron beam is generated by a VHF gun in CW mode with a repetition rate up to about 1 MHz. A superconducting linac with two bunch compressors then accelerates the electron beam to about 8 GeV. The electron beam is used to feed the FEL undulator complex with multi undulator lines, where the X-ray radiations from 0.4-25keV photon energy are generated and amplified to saturation. The FEL undulator complex contains at least three parallel undulator lines, referred to as FEL-I (3-15 keV), FEL-II (0.4-3 keV) and FEL-III (10-25 keV) respectively [2]. In addition, spaces are reserved for future upgrade of more undulator lines.

For the simultaneous operation of several undulator lines with different parameters and operation modes, a set of beam distribution system should be applied between the SRF linac and the undulator lines. The beam distribution system should perform a rapidly, stably, and precisely distribution of the CW electron bunches from linac to each undulator lines in a certain pattern. At the meantime, beam quality from linac should be well retained after passing through the beam distribution system.

GENERAL LAYOUT

The schematic view of the beam distribution section of SHINE is seen in Fig.1. The SRF linac of SHINE is installed near the middle line of linac tunnel and the three undulator lines are installed in two of the three parallel undulator tunnels. FEL-II and FEL-I lie in left and right side respectively of the middle undulator tunnel. FEL-III lies in the left side of the west undulator tunnel. Between the linac tunnel and the undulator tunnels it is the #2 shaft with the main dump of the linac inside. The beam distribution system starts from the end part of the linac tunnel, passes through the #2 shaft and ends at the undulator tunnel. Since all the three undulator lines are not on the same line of the linac, there should be three linac-to-undulator (LTU) branches to deflect the electron beam from the linac to each undulator line. Because of the configuration of the three undulator lines, to avoid the confliction of the three LTU branches, the sequence of them from the end of the linac are LTU-2, LTU-3, LTU-1, respectively.

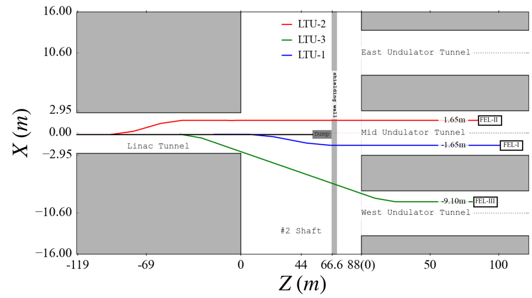

Figure 1: Layout of the beam distribution section of SHINE.

KICKER-SEPTUM SECTION

The beam distribution system of SHINE is designed to perform a bunch-by-bunch and flexible beam separation to the 8 GeV and 1 MHz electron beam. To achieve this goal, the kicker-septum configuration with a set of fast vertical kickers and a DC Lamberson septum magnet should be applied. When the kicker set is on, the electron bunch is kicked vertically. After a certain distance of drift, it is transferred to the DC Lamberson septum magnet with a vertical offset and horizontally deflected by the deflection field region of the septum magnet. When the kicker is off, the electron bunch goes straight to the field free region of the septum magnet and passes through without any deflection.

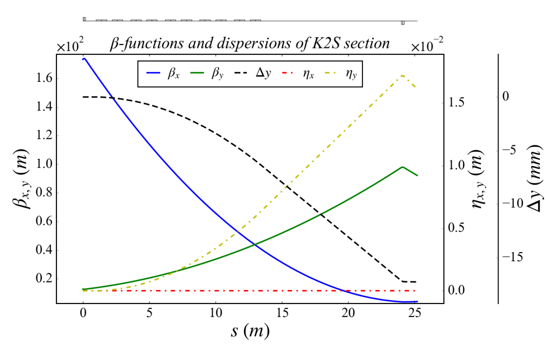

Figure 2: Kicker-septum configuration of SHINE.

Figure 2 shows the optics and beam trajectory of one of such a kicker-septum section. The kicker set deflects the

---

* Work supported by the National Key Research and Development Program of China (No. 2016YFA0401901).

† chensi@zjlab.org.cn

ISBN: 978-3-95450-214-1 ISSN: 2673-5490 doi:10.18429/JACoW-IPAC2021-TUPAB081

electron bunch about 1 mrad in total with an flexible pattern. The vertical separated distance between the kicked and straight bunches at the septum magnet is about 17 mm. The optics of kicker-septum section is designed to have a quite small β_x at the septum for minimizing the CSR effect and a rather small β_y envelop in the kickers region for reducing the influence of kicker field jitter. Because of the limited longitudinal space, the optics of kicker-septum section is designed to be a periodic lattice so that all the three LTU branches have the same kicker-septum configuration.

LINAC-TO-UNDULATOR BRANCHES

General Description

Starting from the end of the linac, the first branch is LTU-2, then LTU-3 and LTU-1 at last. At the entrance of each LTU branch, there is a kicker-septum section as described above. Since all the FEL undulator lines are parallel to the linac line, the three LTU branches should first use a dog-leg to deflect the electron bunches to the designed direction and then match them to the entrance of each undulator line. Each dog-leg consists of two almost identical double-bend achromatic (DBA) sections and a matching section between two DBA sections. The DC Lamberson septum magnet acts as the first dipole magnet of the first DBA of each dog-leg. After the dog-leg, a series of FODO cells with 45° phase advance delivers the electron beam to the entrance of each undulator line. The FODO cells are also used for beam diagnostics and halo collimations. The detailed design of the three LTU branches is described below.

LTU-2

The total deflection angle of LTU-2 is 3.0°. The lattice functions of LTU-2 are shown in Fig. 3. The optics of the dog-leg is designed to be symmetrical and the phase advance of the matching section between two DBA sections is matched to be π for CSR cancellation [3]. After the horizontal dog-leg, a small vertical dog-leg with quadruple magnets is used to compensate the vertical offset and dispersion introduced by the kickers. In order to reduce the microbunching instability effect, a small chicane is used to make the $R_{56} \approx 0$. Then the FODO cells bring the electron beam to the entrance of the undulator line.

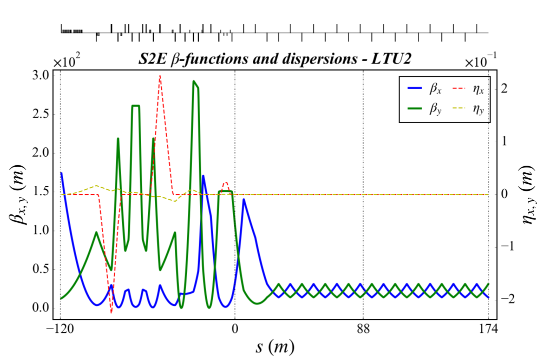

Figure 3: Lattics functions of LTU-2 branch.

LTU-3

The next branch is the LTU-3, which is the longest one among the three branches. Because the FEL-III line is installed in the west undulator tunnel, the horizontal deflection distance of LTU-3 should be about 8.9 m. The dog-leg of LTU-3 starts from the linac tunnel, passes through the #2 shaft and ends at the west undulator tunnel. As is seen in Fig. 1, the geometry of LTU-3 is limited by the structure of the tunnels and #2 shaft. The horizontal deflection part of LTU-3 is also a dog-leg consists of two opposite DBA sections with ±3.6° deflection angle and a long matching section with 3π phase advance. The vertical dog-leg to correct the vertical offset and dispersion will be put at the front part of the long matching section. The lattice functions of LTU-3 are shown in Fig. 4.

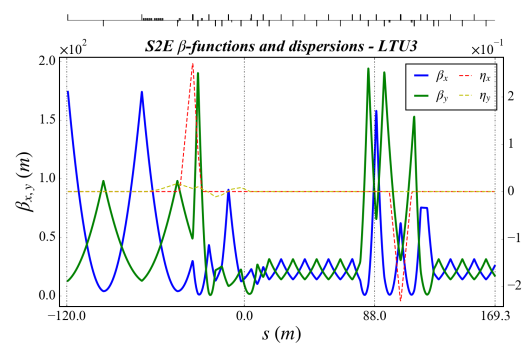

Figure 4: Lattics functions of LTU-3 branch.

LTU-1

The deflection part of the LTU-1 is a pure horizontal dog-leg. The entrance of the DC Lamberson septum is at about 19.5 m downstream the exit of the linac tunnel. The total bending angle of the dog-leg is 2.0°. Such a bending angle is determined by the transverse size of the first quadrupole in the entrance DBA. The total path length of the dog-leg is about 60 m so that the most part of the LTU-1 is inside the #2 shaft. The lattice function of LTU-1 from the entrance of the beam switchyard to the entrance of FEL-I undulator line is shown in Fig. 5.

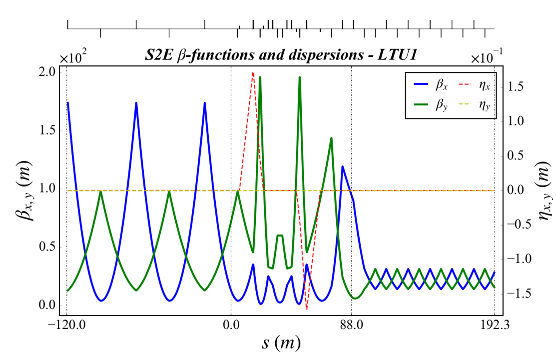

Figure 5: Lattics functions of LTU-1 branch.

ISBN: 978-3-95450-214-1 ISSN: 2673-5490 doi:10.18429/JACoW-IPAC2021-TUPAB081

START-2-END TRACKING

The particle distribution at the entrance of switchyard is generated from the start-to-end simulation of the linac, as is shown in Fig. 6. The simulation is done by the particle tracking code ELEGANT [4].

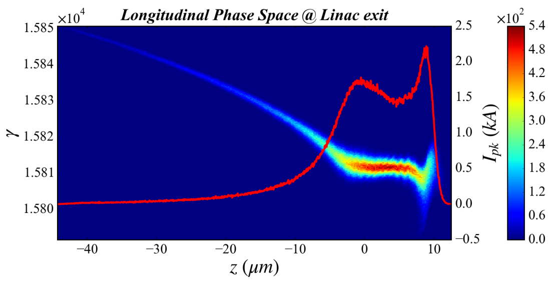

Figure 6: Longitudinal phase space at the exit of linac.

As the main deflection section of the facility, the main beam dynamic issues to be paid special attention during the simulation are the suppression of the CSR induced emittance growth and the microbunching instability. For the suppression of the CSR induced emittance growth, several approaches have been applied in the physics design including the smaller bending angle and optical balance of the lattice. The evolution of the normalized emittance of the three LTU branches is shown in Fig. 7. The tracking results show that the CSR contributed emittance growth is less than 10% for all the three LTU branches.

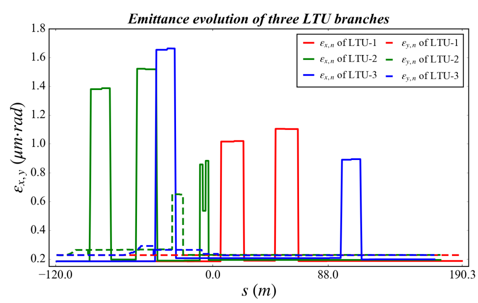

Figure 7: Evolution of emittance along each LTU branch.

Microbunching instability is usually harmful to the FEL process, especially for the undulator line using seeded FEL mechanism, i.e., the FEL-II line. For suppressing the microbunching growth before entering the FEL-II line, the LTU-2 branch is designed to be isochronous. Figure 8 shows a comparison of the current profile at the exit of each LTU branch and the exit of linac. It is seen that the longitudinal phase space is be well kept with such a scheme.

BEAM COLLIMATION

The transverse halo collimation is mainly done in the FODO cells with 45° phase advance and the off-momentum electrons are scraped by the collimator near the peak value of dispersion. The aperture of the collimators should be able to remove the stray electrons as far as possible without reducing the bunch charge too much. The design of the collimator allows the individual collimation of both horizontal and vertical. Each collimator contains two jaws that can be moved independently. This design makes the aperture adjustable in both horizontal and vertical direction for larger energy acceptance. The thickness of the collimator jaws should be sufficient to assure the attenuation of the dark currents. For better absorption of the beam power, water cooling is necessary to the collimator jaws.

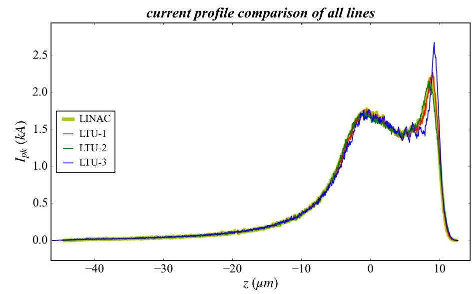

Figure 8: Comparison of the current profile at the exit of each LTU branch.

Another important role of the beam collimation system is the combination with the machine protection system (MPS). In front of the radiation sensitive components, such as the fast kickers and the undulators, there should be collimators for protecting them from the strike of the mis- steering or off-momentum beam while machine failures. The collimator should be able to hold the complete loss of the CW beam in a 100 μs until the beam was shut down. Beam loss monitors should be put close to the collimator to detect such a scenario and connected to the MPS system.

SUMMARY

The beam distribution system of SHINE uses the combination of fast vertical kicker set and DC Lamberson septum to realize the bunch-by-bunch separation of the 1 MHz and 8 GeV electron beam. The lattice of the LTU branch is designed to minimizing the CSR induced emittance growth by minimizing the beam size at each bending magnet and applying the optics balance method. The lattice of LTU-2 is designed to be isochronous in order to avoid micro-bunching growth. The start-to-end tracking simulation is done based on the output of linac simulation. The results show that the emittance and microbunching gain can be well controlled by the present design.

However, because the design of some of the key instruments for beam distribution has not finished yet, the physics design of the beam distribution system is still under iteration. We will upgrade our design in the future.

ACKNOWLEDGEMENTS

This work is supported by the National Key Research and Development Program of China (No. 2016YFA0401901).

ISBN: 978-3-95450-214-1 ISSN: 2673-5490 doi:10.18429/JACoW-IPAC2021-TUPAB081

REFERENCES

[1] C. Feng and H.-X. Deng, "Review of fully coherent free-electron lasers", *Nucl. Sci. Tech.*, vol. 29, p. 160, 2018. doi:10.1007/s41365-018-0490-1

[2] N. Huang *et al.*, "Features and Futures of X-ray Free-Electron Lasers", *The Innovation*, vol. 2, no. 2, p. 100097, 2021. doi:10.1016/j.xinn.2021.100097

[3] S. Di Mitri *et al.*, "Cancellation of Coherent Synchrotron Radiation Kicks with Optics Balance", *Phys. Rev. Lett.*, vol. 110, p. 014801, 2013. doi:10.1103/PhysRevLett.110.014801

[4] M. Borland, "elegant: A Flexible SDDS-Compliant Code for Accelerator Simulation", in *6th International Computational Accelerator Physics Conference (ICAP 2000)*, Darmstadt, Germany, Sep. 2000. doi:10.2172/761286